CHAPTER IV
RESULTS AND DISCUSSION

4.1 Characterization of Organoclays

4.1.1 The Intercalation Effect of Alkylammoniumions Structure

The XRD patterns of the MMT and various surfactant MMT hybrids are shown in Figure 4.1. The XRD curve of MMT had a single peak at 7.04°, corresponding to a basal space of 12.55 Å. The graph also shows that MMT-SA has a single peak at 3.16°, which is equivalent to a basal spacing of 27.94 Å. For MMT-DMS, the XRD curve is split into two peaks, which have 2.15° and 4.37°, corresponding to the basal spaces of 41.06 and 20.20 Å, respectively. MMT-TMS shows two peaks at about 2.25° and 4.28° (39.23 and 20.62 Å). When DMDS is used, the graph has three peaks, 2.37° (37.25 Å), 4.74° (18.63 Å), and 6.91° (12.78 Å).

Figure 4.2 shows the XRD patterns of BEN and various alkylammoniumion BEN hybrids. The XRD curve of BEN has a single peak at 5.92°, corresponding to a basal space of 14.92 Å. BEN-SA shows a single peak at about 3.89° (22.70 Å). For BEN-DMS and BEN-TMS, the XRD curves shows peak at 4.12° and 3.62°, the basal space are 21.43 and 27.94 Å, respectively. The graph of BEN-DMDS has three peaks at 2.47°, 4.59°, and 6.98°, which are equivalent to the basal spacing of 35.74, 19.24, and 12.65 Å, respectively.

Both organo-MMTs and organo-BENs were larger the basal spacing than unmodified MMT and unmodified BEN because of the intercalation of surfactant into the interlayer of clay layers.

Alkylammonium ions could densely pack in the interlayer of MMT. Comparing with BEN, the basal spacing of organo-BENs was less than that of organo-MMTs, further less packing of alkylammonium ions in the interlayer. Because MMT had higher CEC value, further more ion exchange reaction and more surfactant in the interlayer.

For MMT modified with tertiary amine, MMT-DMS appeared two peaks in XRD pattern. This result indicated that there were two forms of surfactant intercalation in the interlayer. Because MMT had higher CEC, further more ion exchange reaction and more surfactant in the interlayer, therefore MMT-DMS had two intercalation forms while BEN-DMS had one intercalation form (BEN-DMS shows only a single peak in XRD pattern). But nanoclays were modified with primary amine did not exhibit this effect, both MMT-SA and BEN-SA showed one peak in XRD pattern.

MMT-TMS appeared two peaks and BEN-TMS showed only one peak in XRD patterns like the cause of nanoclays were modified with DMS. For MMT-DMDS and BEN-DMDS, the XRD curves were split into three peaks. Therefore CEC of nanoclays did not affect on the intercalation forms when nanoclays were modifid with DMDS.

Effect of monoalkyl and dialkyl on nanoclays was considered. Two tails of C_{18} surfactant structure (DMDS) was more effective to intercalate silicate layer when comparing with one tail (TMS).

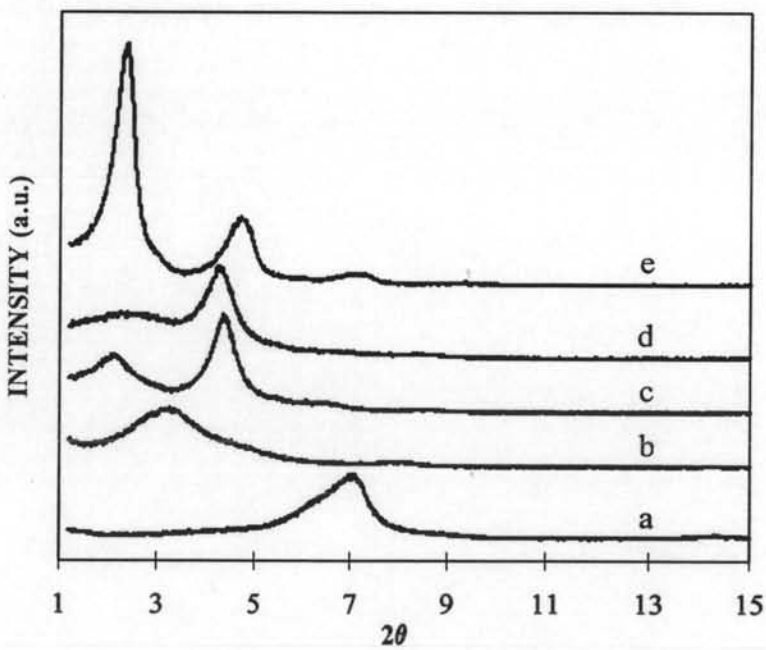

Figure 4.1 XRD patterns of organo-MMTs and unmodified-MMT: a) MMT, b) MMT-SA, c) MMT-DMS, d) MMT-TMS, and e) MMT-DMDS.

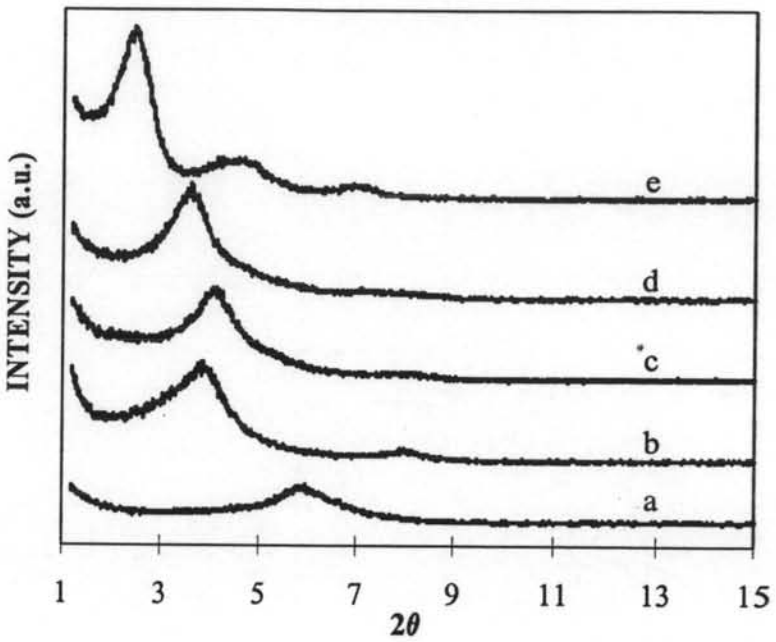

Figure 4.2 XRD patterns of organo-BENs and unmodified-BEN: a) BEN, b) BEN-SA, c) BEN-DMS, d) BEN-TMS, and e) BEN-DMDS.

4.1.2 Thermogravimetric Analysis

The results of the thermogravimetric analysis of organo-MMTs and organo-BENs are shown in Table 4.1. There are three main mass loss steps. For organo-MMTs, the first mass loss step due to dehydration is observed over the temperature range 50.6 to 71.0°C and %mass loss varies from 0.80 up to 3.40%. The second mass loss step due to desurfactant appears at about 256.0-419.3°C and %mass loss varies from 36.80 up to 50.00%. The last step is attributed to dehydroxylation of the structural OH units of clay over the 600.6-633.5°C temperature range. For organo-BENs, the first mass loss step is observed over the temperature range 54.3 to 58.3°C and %mass loss varies from 0.32 up to 4.10%. The second mass loss step appeared at about 240.3-404.6°C and %mass loss varies from 18.80 up to 29.35%. The last step is over the 587.6-688.3°C temperature range.

MMT, the dehydration in the first mass loss step appeared at 96.7°C and 11.40 %mass loss which was higher than organo-MMTs indicate that there were more metal cation in interlayer spacing. For BEN, the dehydration was observed at

94.9°C and 9.70 %mass loss. The same result of reduced %mass loss and reduced temperature were observed in organo-BENs. Decreasing of metal cation in the interlayer caused by ion exchange reaction between metal cation and alkylammonium ions. The second mass loss steps of MMT and BEN were not observed because MMT and BEN did not ion exchange with surfactant. The last step was attributed to dehydroxylation of the structural OH units of MMT slit into two peaks at 669.2 and 770.5°C. The % mass losses were 3.10 and 40.70%. For BEN, the last mass loss step was observed at 668.8°C and %mass loss was 4.20%.

In the desurfactant step of MMT, % mass losses were higher than those in BEN. Because MMT was higher CEC value (115.50 meq/100g) than CEC value of BEN (52.55 meq/100g). More CEC value was more chance to ion exchange reaction between Na^+ and alkylammonium ion resulting in higher weight of surfactant in the interlayer spacing and higher desurfactant temperature.

Table 4.1 Thermogravimetric analysis of MMT, BEN, organoclays (MMT, BEN) for various surfactants

Sample	Dehydration (water absorbed by metal cations)		Desurfactant		Dehydroxylation (the structural OH units)	
	%mass loss	Temp.(°C)	%mass loss	Temp.(°C)	%mass loss	Temp.(°C)
MMT	11.40	96.7	-	-	3.10/0.70	669.2/770.5
MMT- SA	1.10	52.6	38.50	310.7/401.0	2.20	633.5
MMT- DMS	0.80	62.4	38.00	289.6/395.8	1.90	600.6
MMT- TMS	3.40	71.0	36.80	264.5/322.6/419.3	1.90	607.5
MMT- DMDS	2.20	50.6	50.00	256.0/314.0/393.0	1.47	604.3
BEN	9.70	94.9	-	-	4.20	668.8
BEN-SA	0.32	54.3	22.57	249.5/394.9	1.47	592.7
BEN-DMS	1.50	56.4	18.80	240.3/381.7	1.70	587.6
BEN-TMS	4.10	56.6	19.40	262.7/315.9/404.6	1.20/1.60	591.9/688.3
BEN-DMDS	1.68	58.3	29.35	316.3/396.3	2.42	660.7

However the mass of surfactant in the interlayer of organoclays converted into molar of surfactant (Tables 4.2 and 4.3). The exchange molars of

surfactants in organo-MMTs were higher than those in organo-BENs. These results were attributed to more ion exchange reaction in the interlayer of MMT due to MMT had higher CEC value.

The exchange molars of surfactants decreased in order of organomodified nanoclays with SA > DMS > TMS > DMDS, respectively. This effect was similar in organo-MMTs and organo-BENs. These results indicated that the exchange molar content of surfactant decreased with the molecular weights of surfactant increased. The same result was observed by Lee J.Y. and Lee H.K (2004) who modified montmorillonite-rich clay with 99% purity and it was modified with many cationic organic surfactants. The exchanged content of the organic surfactants decreased with the increment of molecular weight of the organic surfactants.

Table 4.2 The exchanged molar content of surfactants in organo-MMTs

Sample	MMT-SA	MMT-DMS	MMT-TMS	MMT-DMDS
The exchanged molar (mole)	0.144	0.135	0.118	0.096

Table 4.3 The exchanged molar content of surfactants in organo-BENs

Sample	BEN-SA	BEN-DMS	BEN-TMS	BEN-DMDS
The exchanged molar (mole)	0.085	0.067	0.062	0.056

Table 4.4 shows the decomposition temperatures of SA, DMS, TMS and DMDS which were 243.8, 268.0, 271.1, and 353.4°C, respectively. The surfactant with higher molecular weight had higher decomposition temperatures. For MAA, the degradation temperature was 144.2°C.

Table 4.4 Decomposition temperatures of surfactants and MAA

Sample	SA	DMS	TMS	DMDS	MAA
Degradation Temperature (T_d)	243.8	268.0	271.1	353.4	144.2

4.2 Characterization of Modified Organoclays

4.2.1 The Intercalation Effect of Co-Intercalation Monomer

The XRD patterns in Figure 4.3, the shifted peaks of modified organo-MMTs into lower angle indicate that the basal spacing values of them are higher than those of organo-MMTs (Table 4.5). These results were clear in modified organo-BENs, their basal spacing are shown in Table 4.6 (The XRD patterns show in Figure 4.4). MMA easily intercalated into clay layer, further increasing the interlayer distance.

MMA could be swollen into the interlayer due to its strong polarity. The strong hydrogen bonding between COOH group from MMA and the oxygen groups of silicate layers was occurred.

The same phenomenon was investigated by Liu X. and Wu Q. (2001). They modified organoclay with epoxypropyl methacrylate which had a larger interlayer spacing than organophilic clay modified by alkyl ammonium. Furthermore, Zhang Y.-Q. *et al.* (2004) carried out modified organoclay. The organoclay was first modified with maleic anhydride (MA) in solution with a small quantity of a co-swelling agent and an initiator. The XRD patterns showed that the basal distance in the MA-modified organoclay was 30 nm, which was larger than that of the original organoclay (19.6 nm).

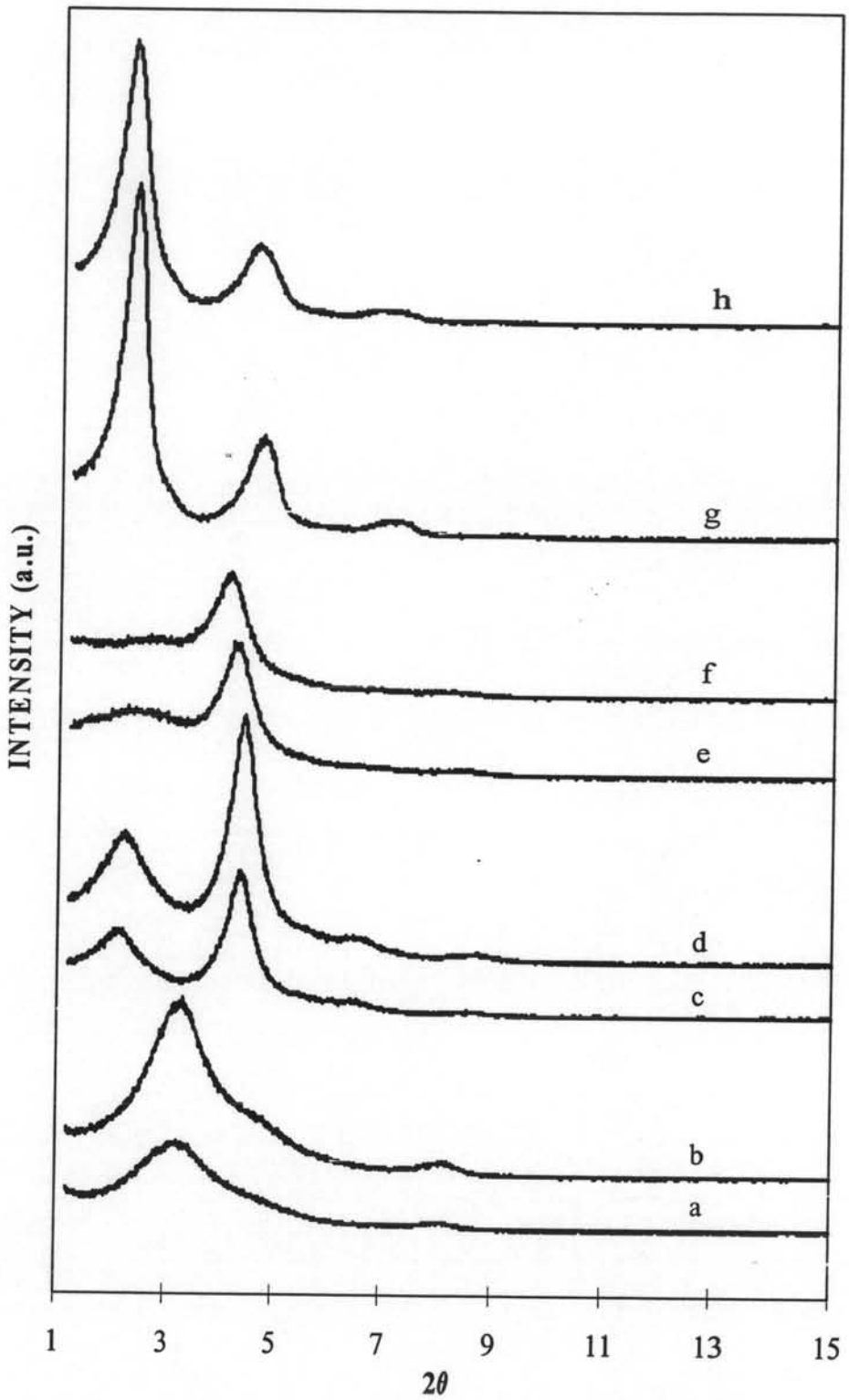

Figure 4.3 XRD patterns of organo-MMTs and modified organo-MMTs: a) MMT-SA, b) MMT-SA/MAA, c) MMT-DMS, d) MMT-DMS/MAA, e) MMT-TMS, f) MMT-TMS/MAA, g) MMT-DMDS, and h) MMT-DMDS/MAA.

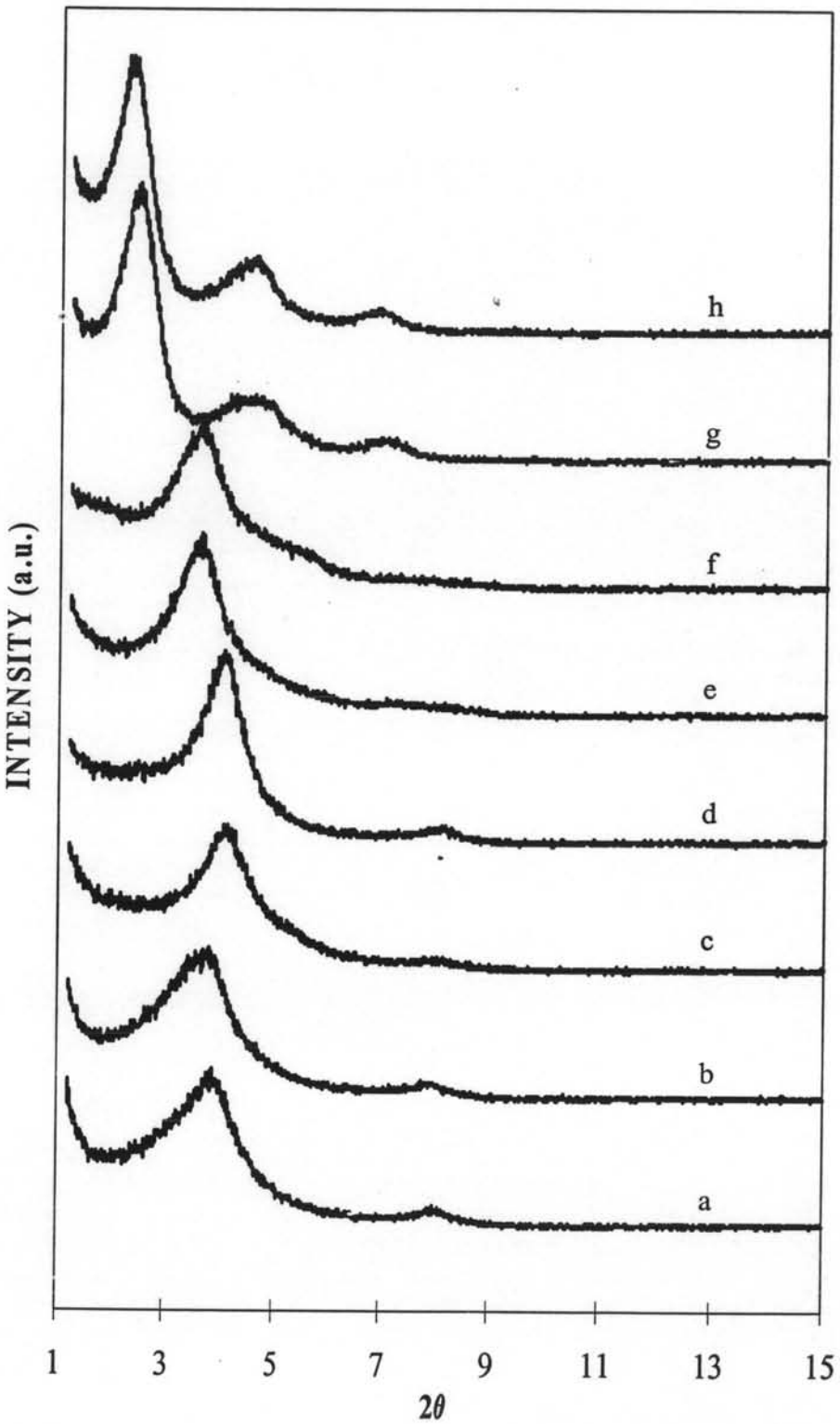

Figure 4.4 XRD patterns of organo-BENs and modified organo-BENs: a) BEN-SA, b) BEN-SA/MAA, c) BEN-DMS, d) BEN-DMS/MAA, e) BEN-TMS, f) BEN-TMS/MAA, g) BEN-DMDS, and h) BEN-DMDS/MAA.

Table 4.5 The basal spacing of modified organo-MMTs

Sample	MMT-SA/MAA	MMT-DMS/MAA	MMT-TMS/MAA	MMT-DMDS/MAA
Basal spacing (Å)	27.76	39.58/19.93	31.98/21.22	37.89/19.19/12.89

Table 4.6 The basal spacing of modified organo-BENs

Sample	BEN-SA/MAA	BEN-DMS/MAA	BEN-TMS/MAA	BEN-DMDS/MAA
Basal spacing (Å)	23.67	21.59	24.73	38.72/19.24/12.74

4.2.2 Thermogravimetric Analysis

The results of the thermogravimetric analysis of modified organo-MMTs and modified organo-BENs are shown in Table 4.7. For modified organo-MMTs, the first mass loss step is observed over the temperature range 64.6 to 68.6°C and %mass loss varies from 0.30 up to 3.80%. The second mass loss step due to desurfactant appears at about 238.2-422.3°C and %mass loss varies from 36.70 up to 49.10%. The last step is attributed to dehydroxylation of the structural OH units of clay over the 595.2-608.8°C temperature range. For modified organo-BENs, the first mass loss step is observed over the temperature range 52.8 to 58.4°C and %mass loss varies from 0.43 up to 3.80%. The second mass loss step appeared at about 237.8-401.5°C and %mass loss varies from 19.90 up to 32.36%. The last step is over the 559.6-688.3°C temperature range.

The higher %mass loss in desurfactant step of modified organo-BENs and modified organo-MMTs was observed, due to the addition of MMA into the interlayer, except MMT-TMS/MAA and MMT-DMDS/MAA which % mass loss only slightly decreased at desurfactant step.

Table 4.7 Thermogravimetric analysis of MMT, BEN, organoclays (MMT, BEN) and modified organoclays (MMT, BEN) for various surfactants

Sample	Dehydration (water absorbed by metal cations)		Desurfactant		Dehydroxylation (the structural OH units)	
	%mass loss	Temp.(°C)	%mass loss	Temp.(°C)	%mass loss	Temp.(°C)
MMT-SA/MAA	0.30	68.6	38.90	238.2/313.1/398.0	2.20	600.8
MMT- DMS/MAA	0.60	65.5	38.90	287.0/394.9	1.80	608.8
MMT- TMS/MAA	3.80	67.9	35.70	263.8/325.2/422.3	1.90	602.6
MMT- DMDS/MAA	1.40	64.6	49.10	259.0/320.4/401.1	1.50	595.2
BEN-SA/MAA	0.43	52.8	23.44	242.1/388.4	1.40	581.3
BEN-DMS/MAA	1.70	56.0	20.10	239.1/375.6	1.70	581.4
BEN-TMS/MAA	3.80	58.4	19.90	245.6/315.3/401.5	1.40/1.20	559.6/683.3
BEN-DMDS/MAA	1.78	57.8	32.36	237.8/315.1/397.4	1.90	650.2

4.3 Characterization of PP/Clays Nanocomposites

4.3.1 Dispersion of Silicate Layer Structure

The XRD patterns of PP/organoclays nanocomposites are shown in Figures 4.5 and 4.6. Table 4.8 and 4.9 show their basal spacing. According to Figure 4.5 the XRD curves of PP-MMT-SA/MAA 3% and PP-MMT-DMS/MAA 3%, have a single peak at 3.17°and 4.48°, corresponding to a basal space of 27.85 and 19.71Å, respectively. For PP-MMT-TMS/MAA 3%, the XRD curve is split into two peaks, which have 2.46° and 4.18°, corresponding to the basal spaces of 35.88 and 21.12Å. PP-MMT-DMDS/MAA 3% shows two peaks at about 2.34° and 4.57° (37.72 and 19.32 Å).

Figure 4.6, PP-BEN-SA/MAA 3% and PP-BEN-DMS/MAA 3% show a single peak at about 2.82° (31.30 Å) and 3.79° (23.29 Å), respectively. For BEN-TMS/MAA 3% and PP-BEN-DMDS/MAA 3%, the XRD curves show peak at 2.88°/4.19° (30.65/21.07 Å), and 2.28°/4.61° (38.71/19.15 Å), respectively.

PP/MMT nanocomposites, which modified with SA/MAA, DMS/MAA, and TMS/MAA, their basal spacing were larger and their board peaks

were observed. These results indicated that grafting reaction could occur. For nanocomposites of modified MMT with DMDS/MAA were not significant the shift of peaks, thereby the structure of surfactant might disturb the grafting reaction.

In PP/BEN nanocomposites, the results were the same as PP/MMT nanocomposites. The grafting reaction was clear in nanocomposites of modified BEN with SA/MAA, DMS/MAA, and TMS/MAA, their peaks were shifted into lower angle and board peaks were obtained. For nanocomposites of modified BEN with DMDS/MAA were not significant increased the basal spacing (Table 4.9) but the peak was board, so the structure of surfactant might interfere the grafting reaction.

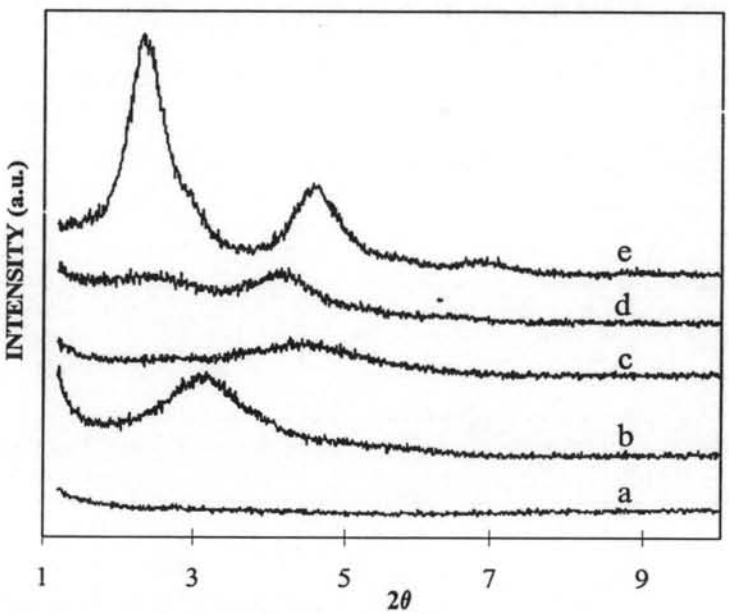

Figure 4.5 XRD patterns of PP/MMT nanocomposites: a) PP-PP/DCP, b) PP-MMT-SA/MAA 3%, c) PP-MMT-DMS/MAA 3%, d) PP-MMT-TMS/MAA 3%, and e) PP-MMT-DMDS/MAA 3%.

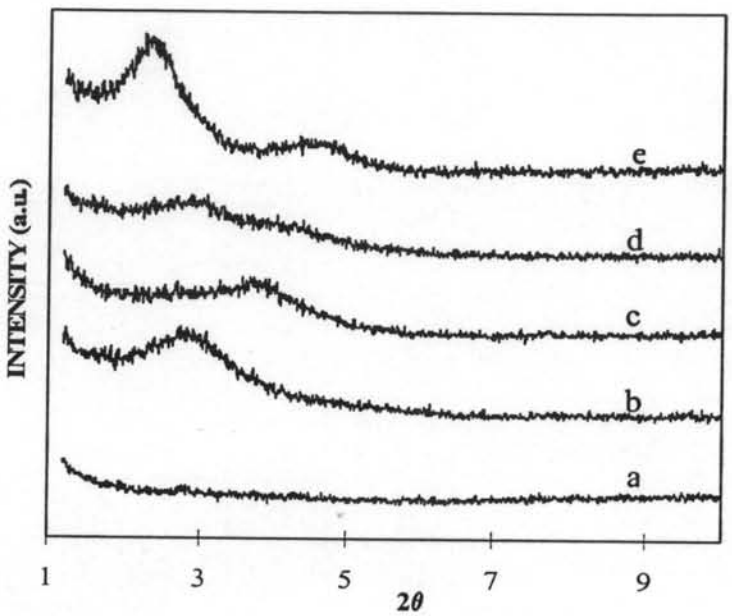

Figure 4.6 XRD patterns of PP/BEN nanocomposites: a) PP-PP/DCP, b) PP-BEN-SA/MAA 3%, c) PP-BEN-DMS/MAA 3%, d) PP-BEN-TMS/MAA 3%, and e) PP-BEN-DMDS/MAA 3%.

Table 4.8 The basal spacing of modified organo-MMTs and PP/clays nanocomposites

Materials	Basal spacing (Å)	
	Modified Oranoclays	PP/clays nanocomposites
MMT-SA/MAA	27.76	27.85
MMT-DMS/MAA	39.58/19.93	19.71
MMT-TMS/MAA	31.98/21.22	35.88/21.12
MMT-DMDS/MAA	37.89/19.19/12.89	37.72/19.32

Table 4.9 The basal spacing of modified organo-BENs and PP/clays nanocomposites

Materials	Basal spacing (Å)	
	Modified Oranoclays	PP/clays nanocomposites
BEN-SA/MAA	23.67	31.30
BEN-DMS/MAA	21.59	23.29
BEN-TMS/MAA	24.73	30.65/21.07
BEN-DMDS/MAA	38.72/19.24/12.74	38.71/19.15

The effect of different nanoclays (BEN and MMT) on dispersion of silicate clay layers in nanocomposites was investigated. BEN had lower polarity than MMT, thereby BEN could well disperse in PP matrix which is a polymer with low polarity. These results were confirmed by the board peaks of XRD patterns.

4.3.2 Thermogravimetric Analysis

Table 4.10 shows the decomposition temperatures (T_d) of PP/clay nanocomposites which were determined by thermogravimetric analysis. Decomposition temperature of PP-PP/DCP was 422.4°C. The increased decomposition temperatures indicated that MMT had thermal stability effect in the PP matrix. T_d of PP-MMT-SA/MAA 3% (organomodification MMT with primary amine) was lower than that of PP-MMT-DMS/MAA 3% (organomodification MMT with teriary amine). Similarly, T_d of PP-MMT-TMS/MAA 3% (organomodification MMT with monoalkylammonium ion) was lower than that of PP-MMT-DMDS/MAA 3% (organomodification with MMT dialkylammonium ion).

There results were similar to PP/modified organo-BENs nanocomposites. BEN had thermal stability effect in the PP matrix. This result was confirmed by the increased decomposition temperatures of PP/BEN nanocomposites.

T_d of PP-BEN-DMS/MAA 3% (organomodification BEN with tertiary amine) was higher than that of PP-BEN-SA/MAA 3% (organomodification BEN with primary amine). The T_d of nanocomposites organomodified BEN with dialkylammonium ion was higher than that organomodified BEN with monoalkylammonium ion.

Td of PP/clay nanocomposites increased in order of modified nanoclays with SA/MAA > DMS/MAA > TMS/MAA > DMDS/MAA, respectively. The nanocomposites of modified nanoclays with higher molecular weight of surfactant had the increased decomposition temperatures. This effect was similar in nanocomposites of MMT and BEN.

Table 4.10 Decomposition temperatures of PP/clays nanocomposites

Nanocomposites	T_d (°C)	
	Montmorillonite	Bentonite
PP-SA/MAA 3%	428.6	429.3
PP-DMS/MAA 3%	429.4	432.9
PP-TMS/MAA 3%	435.0	433.5
PP-DMDS/MAA 3%	441.2	436.0

4.3.3 Crystallization of PP/Clays Nanocomposites

Differential Scanning Calorimeter (DSC) scans at cooling rate 10°C/min was used to observe the crystallization temperature. The crystallization temperatures (T_c) of PP/clays nanocomposites are shown in Figure 4.7 and Figure 4.8. Figure 4.7 shows T_c of PP/PP-DCP, PP-MMT-SA/MAA 3%, PP-MMT-DMS/MAA 3%, PP-MMT-TMS/MAA 3% and PP-MMT-DMDS/MAA 3% which were 108.8, 111.1, 109.8, 110.5, and 110.0°C, respectively. The addition of modified

organo-MMTs into the PP matrix resulted in a slight increase of crystallization temperature of the polymer matrix. The observed increase in crystallization temperature could be attributed to the modified organo-MMTs acting as a nucleating agent in PP.

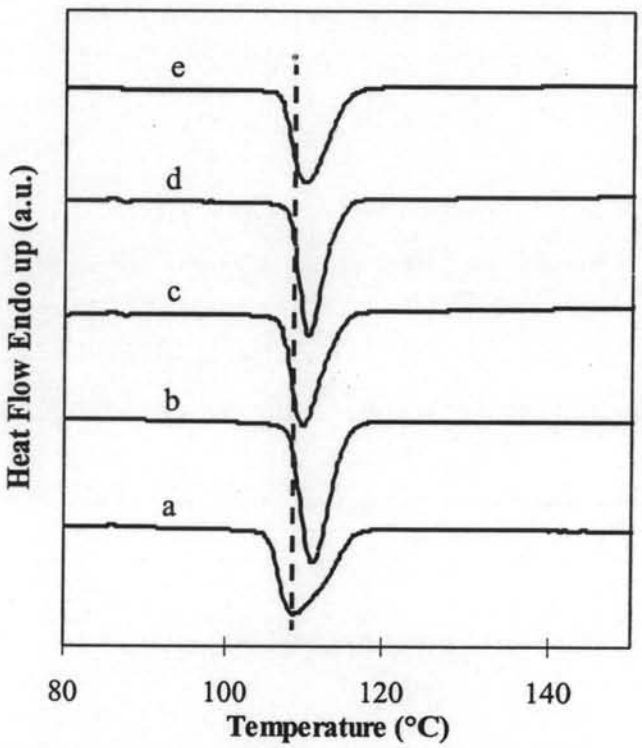

Figure 4.7 DSC cooling scan thermograms of PP/MMT nanocomposites: a) PP-PP/DCP, b) PP-MMT-SA/MAA 3%, c) PP-MMT-DMS/MAA 3%, d) PP-MMT-TMS/MAA 3%, and e) PP-MMT-DMDS/MAA 3%.

PP/BEN nanocomposites presented the same result as PP/MMT nanocomposites. Crystallization temperatures of PP-BEN-SA/MAA 3%, PP-BEN-DMS/MAA 3%, BEN-TMS/MAA 3%, and PP-BEN-DMDS/MAA 3% were 112.3, 113.5, 113.1, and 111.3°C, respectively (Figure 4.8). The modified organo-BENs could act as the nucleating agent better than the modified organo-MMTs due to nanocomposites of modified organo-BENs had higher T_c.

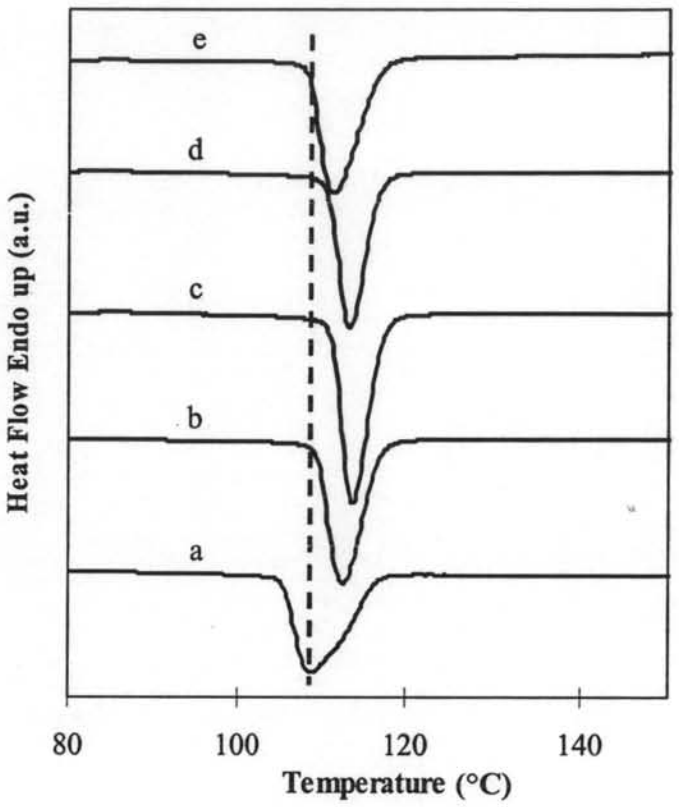

Figure 4.8 DSC cooling scan thermograms of PP/BEN nanocomposites: a) PP-PP/DCP, b) PP-BEN-SA/MAA 3%, c) PP-BEN-DMS/MAA 3%, d) BEN-TMS/MAA 3%, and e) PP-BEN-DMDS/MAA 3%.

The crystal structures of PP/modified organo-MMTs nanocomposites and PP/modified organo-BENs nanocomposites are shown in Figures 4.9 and 4.10, respectively. Both PP/modified organo-MMTs nanocomposites and PP/modified organo-BENs nanocomposites had the same crystal structures as PP-PP/DCP, as confirmed by X-ray Diffractometer (XRD). The results were confirmed by there is no obvious different peak in XRD patterns. The addition of modified organo-MMTs and modified organo-BENs did not affect the crystal structure of the PP matrix.

The crystal structures of PP/clay nanocomposites were determined by XRD. The experiments were operated at a scan speed of 5 degree/min with the 0.02-degree 2θ-stepwise increment. The standard sample holders were applied to PP/clays nanocomposite films.

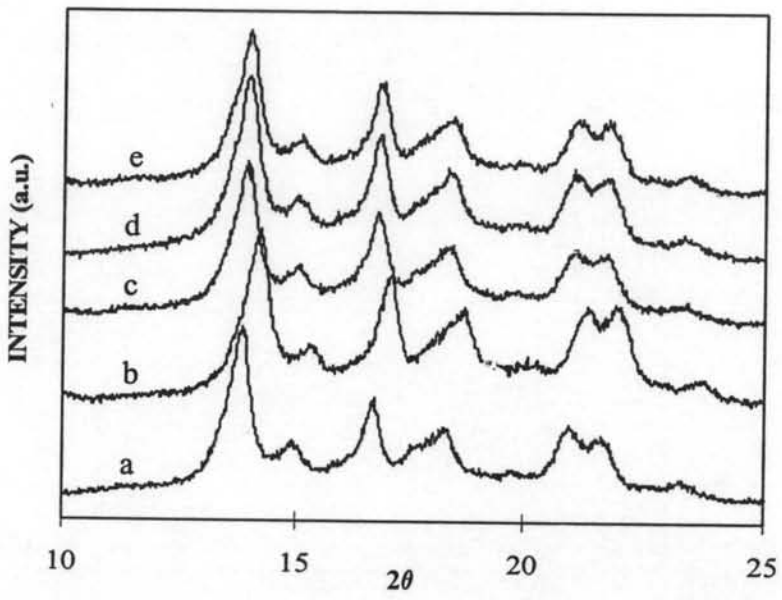

Figure 4.9 Crystal structures of PP/MMT nanocomposites: a) PP-PP/DCP, b)PP-MMT-SA/MAA 3%, c) PP-MMT-DMS/MAA 3%, d) PP-MMT-TMS/MAA 3%, and e) PP-MMT-DMDS/MAA 3%.

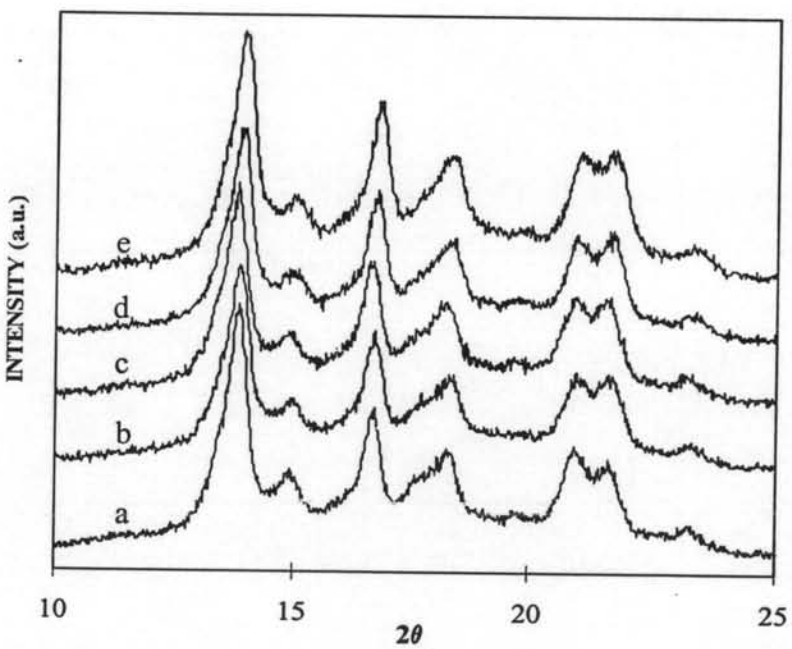

Figure 4.10 Crystal structures of PP/BEN nanocomposites: a) PP-PP/DCP, b) PP-BEN-SA/MAA 3%, c) PP-BEN-DMS/MAA 3%, d) PP-BEN-TMS/MAA 3%, and d) PP-BEN-DMDS/MAA 3%.

Melting temperatures (T_m) of PP/modified organo-MMTs nanocomposites and PP/modified organo-BENs nanocomposites are shown in Figures 4.11 and 4.12, respectively. PP/modified organo-MMTs nanocomposites had the same melting temperature as PP-PP/DCP. The melting temperatures (T_m) of PP/PP-DCP, PP-MMT-SA/MAA 3%, PP-MMT-DMS/MAA 3%, PP-MMT-TMS/MAA 3% and PP-MMT-DMDS/MAA 3% were 156.5, 156.5, 156.0, 155.9, and 155.9°C, respectively. The modified organo-MMTs did not result in any significant change in the melting temperature of the PP matrix.

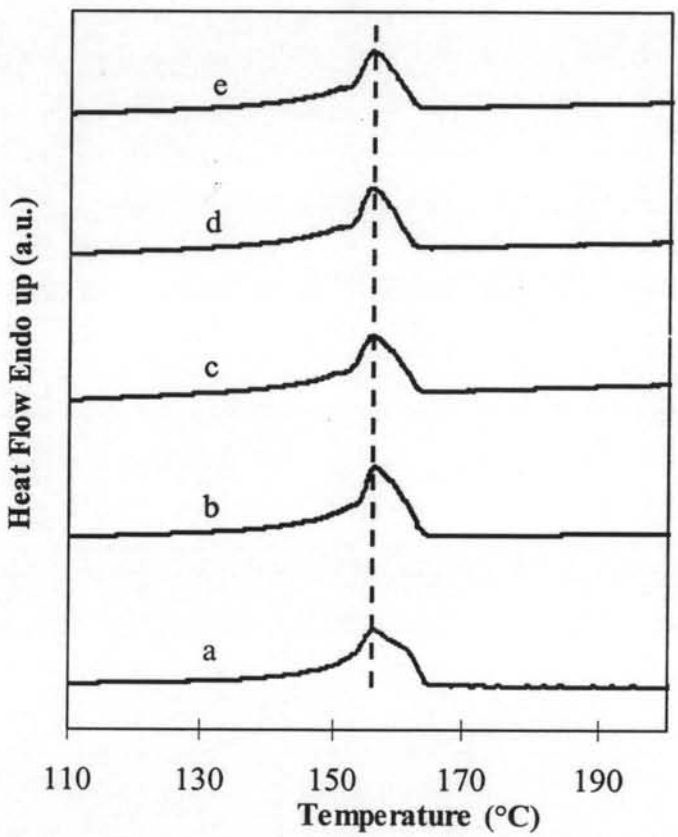

Figure 4.11 DSC heating scan thermograms of PP/MMT nanocomposites: a) PP-PP/DCP, b) PP-MMT-SA/MAA 3%, c) PP-MMT-DMS/MAA 3%, d) PP-MMT-TMS/MAA 3%, and e) PP-MMT-DMDS/MAA 3%.

The melting temperatures of PP-BEN-SA/MAA 3%, PP-BEN-DMS/MAA 3%, BEN-TMS/MAA 3%, and PP-BEN-DMDS/MAA 3% were 156.9,

157.7, 157.4, and 157.7°C, respectively. The higher T_m of PP/modified organo-BENs nanocomposites indicated that PP/modified organo-BENs nanocomposites were better crystal structures.

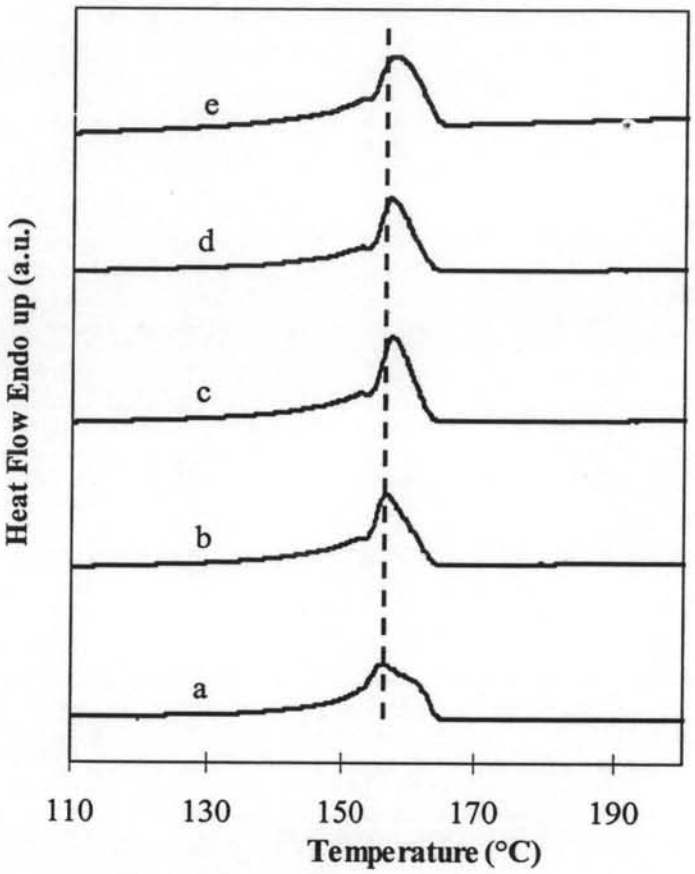

Figure 4.12 DSC heating scan thermograms of PP/BEN nanocomposites: a) PP-PP/DCP, b) PP-BEN-SA/MAA 3%, c) PP-BEN-DMS/MAA 3%, d) PP-BEN-TMS/MAA 3%, and e) PP-BEN-DMDS/MAA 3%.

The amount of crystallinity in PP/clays nanocomposites was investigated (Table 4.11). %Crystallinity of PP-PP/DCP was 29.49% J/g. Both PP/modified organo-MMTs nanocomposites and PP/modified organo-BENs nanocomposites were higher %crystallinity than PP matrix. Thereby modified organo-MMTs and modified organo-BENs affected on increased amount of crystal in PP matrix. These results were attributed to higher T_c of PP/clays nanocomposites.

Table 4.11 %Crystallinity values of PP/clays nanocomposites

Nanocomposites	%Crystallinity	
	Montmorillonite	Bentonite
PP-SA/MAA 3%	31.21	41.75
PP-DMS/MAA 3%	30.53	40.26
PP-TMS/MAA 3%	30.98	38.58
PP-DMDS/MAA 3%	32.21	39.46

%Crystallinity of PP/modified organo-MMTs nanocomposites were less than those of PP/modified organo-BENs nanocomposites. This effect was the same opinion with DSC results.

4.3.4 Melt Flow Index of PP/Clays Nanocomposites

Figure 4.13 shows melt flow index of PP/clays nanocomposites. The MFI of PP-PP/DCP was 24.67 g/10 min. Both PP/modified organo-MMTs nanocomposites and PP/modified organo-BENs nanocomposites had the MFI less than PP-PP/DCP. The MFI of PP-MMT-SA/MAA 3%, PP-MMT-DMS/MAA 3%, PP-MMT-TMS/MAA 3% and PP-MMT-DMDS/MAA 3% which were 22.72, 15.79, 18.79, and 23.60 g/10 min, respectively. And the MFI of PP-BEN-SA/MAA 3%, PP-BEN-DMS/MAA 3%, BEN-TMS/MAA 3%, and PP-BEN-DMDS/MAA 3% were 23.32, 22.57, 17.75, and 23.57 g/10 min, respectively. There results indicated that modified organo-MMTs and modified organo-BENs were the thickening agents.

Silicate layers which were dispersed in the PP matrix could disturb the movement of PP chains. This phenomenon affected on MFI of PP/clays nanocomposites which were shifted to lower values.

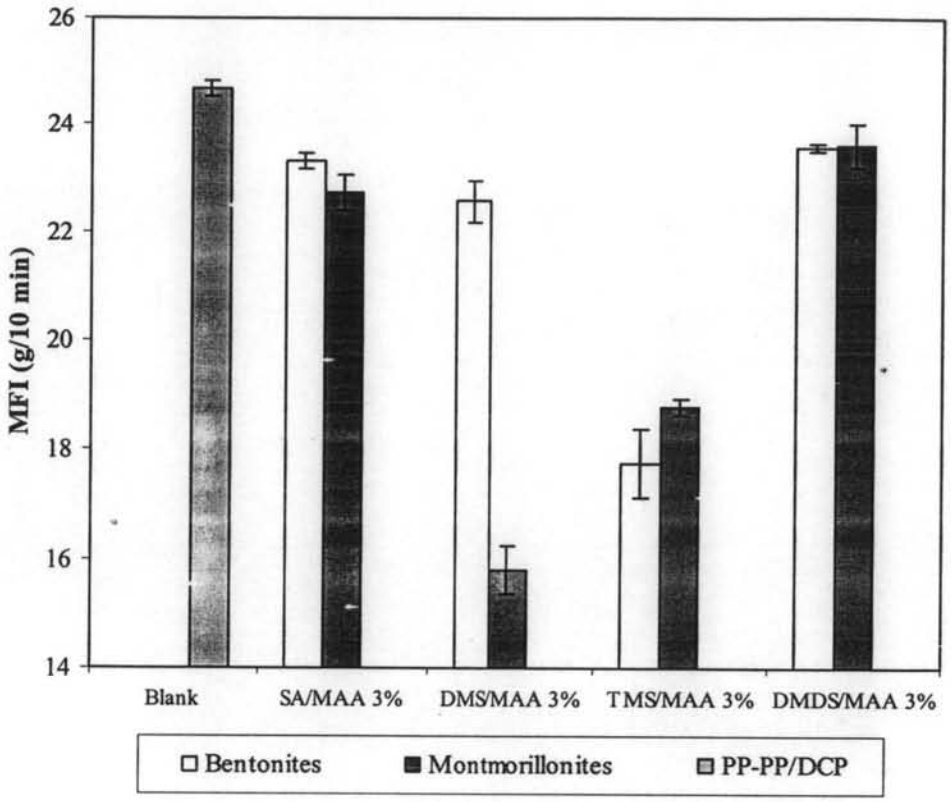

Figure 4.13 MFI of PP/clays nanocomposites.

4.3.5 Mechanical Properties of PP/Clays Nanocompsites

Figure 4.15 shows the tensile strengths of PP-PP/DCP, PP-MMT-SA/MAA 3%, PP-MMT-DMS/MAA 3%, PP-MMT-TMS/MAA 3% and PP-MMT-DMDS/MAA 3% are 35.22, 35.99, 35.13, 35.48, and 35.84 MPa, respectively. And the tensile strength of PP-BEN-SA/MAA 3%, PP-BEN-DMS/MAA 3%, BEN-TMS/MAA 3%, and PP-BEN-DMDS/MAA 3% are 36.34, 36.19, 36.15, and 36.33 MPa, respectively. The tensile strengths of PP/modified organo-MMTs nanocomposites were slightly higher than PP-PP/DCP, except PP-MMT-DMS/MAA 3%. For PP/modified organo-BENs nanocomposites, their tensile strengths were higher than PP-PP/DCP and nanocomposites of modified organo-MMTs. These results were attributed to better crystal structure and the higher % crystallinity of PP/modified organo-BENs nanocomposites.

The tensile modulus of PP/clays nanocomposites are shown in Figure 4.16. The tensile modulus of PP-PP/DCP, PP-MMT-SA/MAA 3%, PP-MMT-

DMS/MAA 3%, PP-MMT-TMS/MAA 3% and PP-MMT-DMDS/MAA 3% are 1915.56, 2241.44, 2230.80, 2702.66, and 2518.28 MPa, respectively. And the tensile modulus of PP-BEN-SA/MAA 3%, PP-BEN-DMS/MAA 3%, BEN-TMS/MAA 3%, and PP-BEN-DMDS/MAA 3% are 1789.76, 1667.82, 1804.36, and 2270.42 MPa, respectively. The tensile modulus of PP/modified organo-MMTs nanocomposites were higher than PP-PP/DCP. For PP/modified organo-BENs nanocomposites, the tensile modulus of PP/modified organo-BENs nanocomposites except PP-BEN-DMDS/MAA 3% were lower than PP-PP/DCP. These results caused by the commercial montmorillonite had very high purity, being very homogeneous. But the commercial sodium activated bentonite, was a low purity bentonite, which had many impurity (saponite, quartz, calcite). The impurities can be found, which act as stress concentrators, allowing crack initiation and propagation, decreasing modulus of the nanocomposite (resemblance with García-López *et al.*).

Figure 4.17 shows strain at break of PP/clays nanocomposites. Strain at break of PP-PP/DCP was the highest (395.93%). The strain at break of PP-MMT-SA/MAA 3%, PP-MMT-DMS/MAA 3%, PP-MMT-TMS/MAA 3% and PP-MMT-DMDS/MAA 3% were 20.04, 24.44, 17.38, and 16.06%, respectively. And the strain at break of PP-BEN-SA/MAA 3%, PP-BEN-DMS/MAA 3%, BEN-TMS/MAA 3%, and PP-BEN-DMDS/MAA 3% were 15.50, 16.04, 16.55, and 24.84%, respectively. Hasegawa N. *et al.* (1998) also reported on the decreased strains of nanocomposite. The elongations of the PP-clay hybrids were smaller than that of PP. The PP-clay hybrids exhibited brittle fracture. Therefore the addition of modified organo-MMTs and modified organo-BENs could decrease the strain at break of PP matrix. Because the dispersion of silicate clay layer in PP matrix could disturb the movement of PP backbone, decreasing strains at break of nanocomposites.

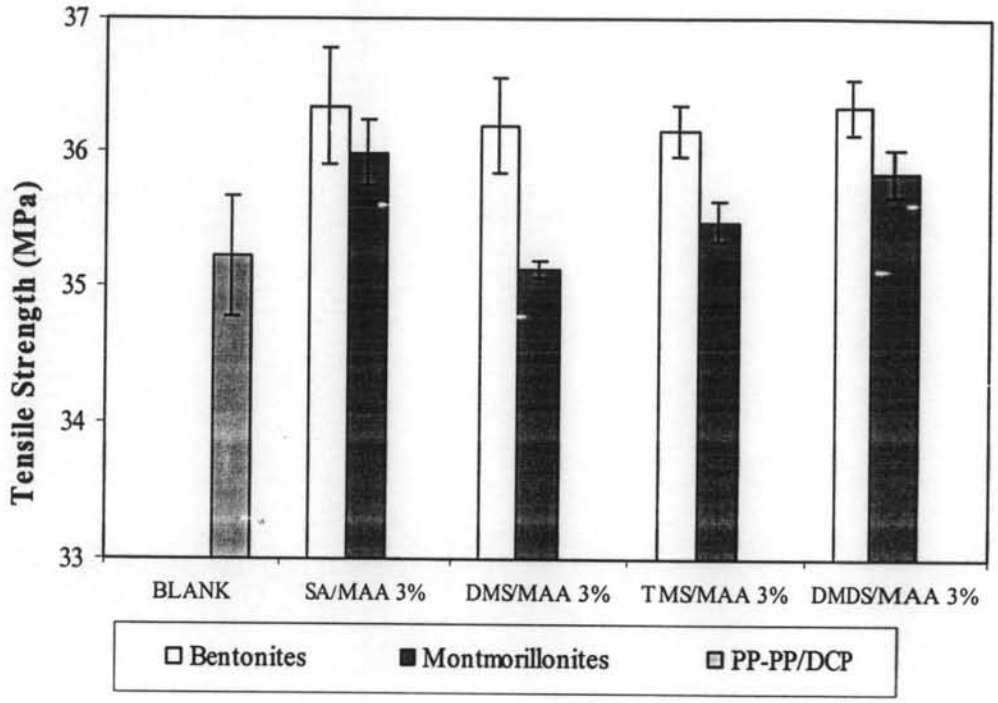

Figure 4.14 Tensile strengths of PP/clays nanocomposites.

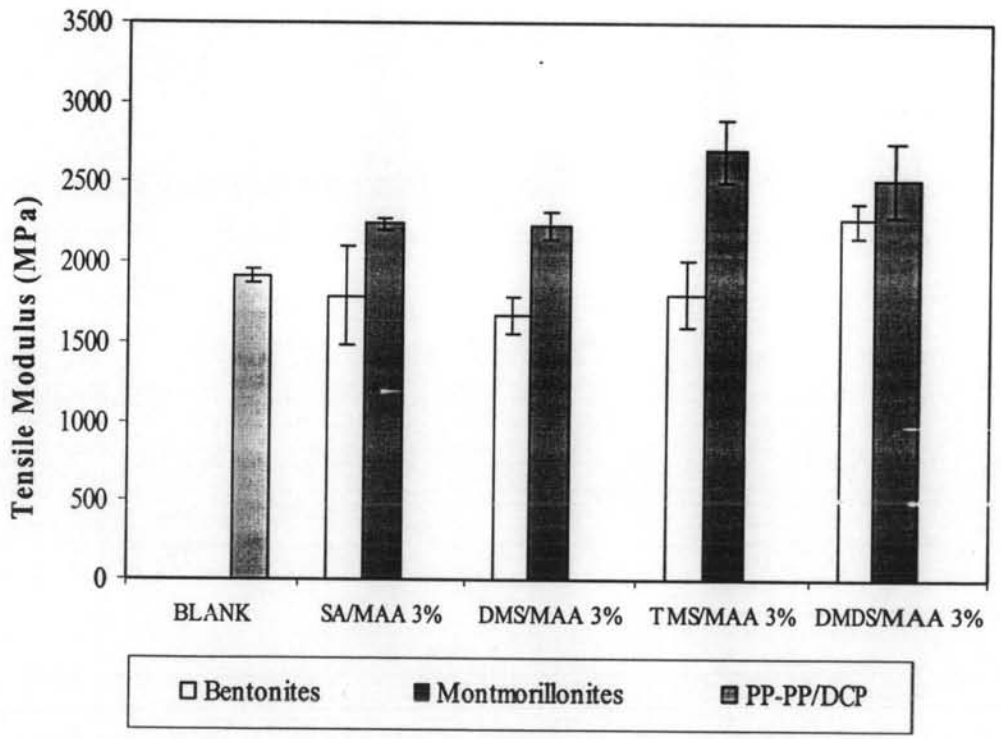

Figure 4.15 Tensile modulus of PP/clays nanocomposites.

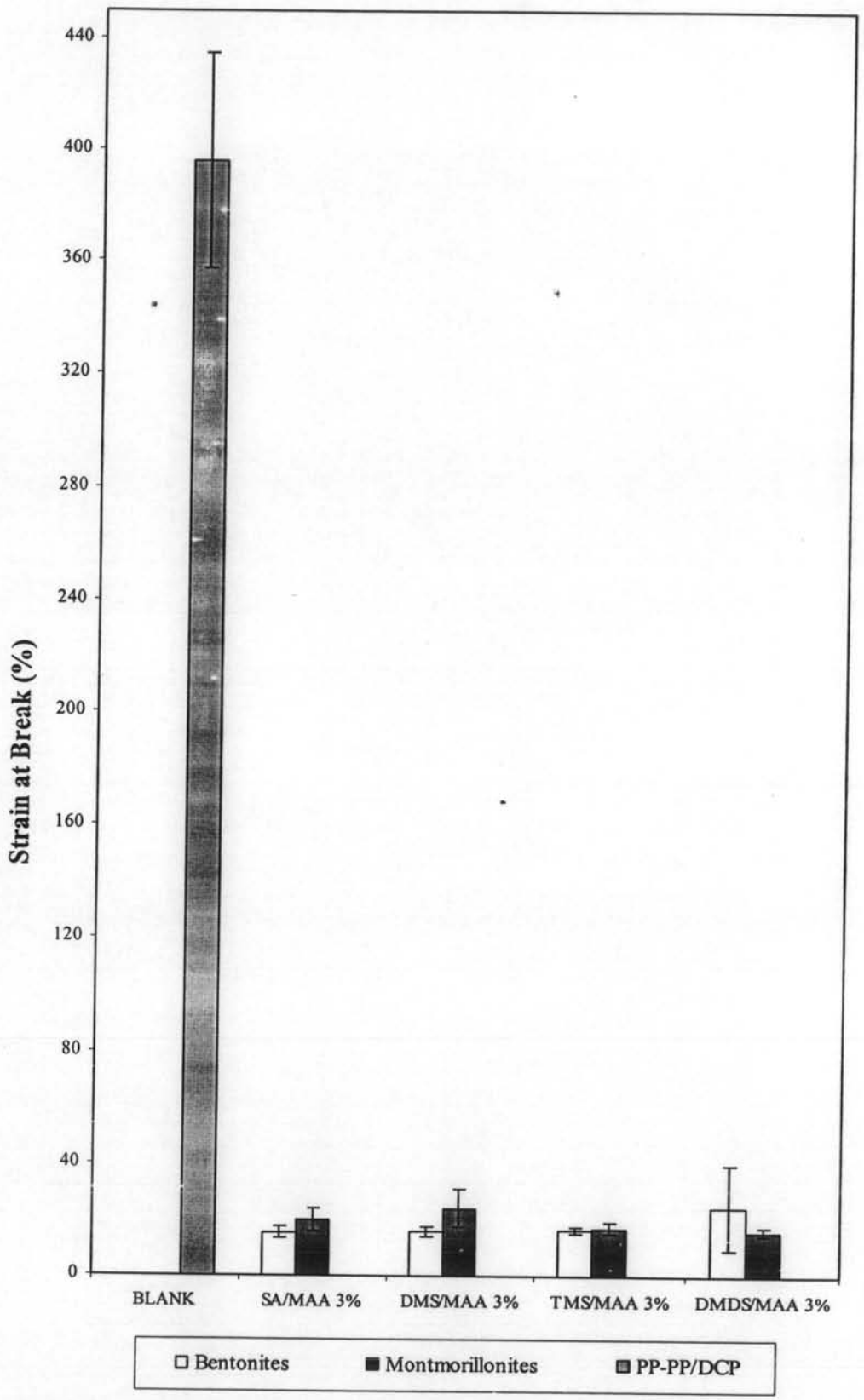

Figure 4.16 Strains at break of PP/clays nanocomposites.